Spontaneous breaking of time-reversal symmetry in the orbital channel for the boundary Majorana flat bands

2013 New J. Phys. 15 085002

(http://iopscience.iop.org/1367-2630/15/8/085002)

New Journal of Physics
The open access journal for physics

Spontaneous breaking of time-reversal symmetry in the orbital channel for the boundary Majorana flat bands

Yi Li, Da Wang and Congjun Wu
Department of Physics, University of California, San Diego, CA 92093, USA
E-mail: y4li@physics.ucsd.edu, d6wang@ucsd.edu and wucj@physics.ucsd.edu

New Journal of Physics **15** (2013) 085002 (10pp)
Received 11 May 2013
Published 5 August 2013
Online at http://www.njp.org/
doi:10.1088/1367-2630/15/8/085002

Abstract. We study the boundary Majorana modes for the single component p-wave weak topological superconductors or superfluids, which form zero energy flat bands protected by time-reversal symmetry in the orbital channel. However, due to the divergence of density of states, the band flatness of the edge Majorana modes is unstable under spontaneously generated spatial variations of Cooper pairing phases. Staggered current loops appear near the boundary and thus time-reversal symmetry is spontaneously broken in the orbital channel. This effect can appear in both condensed matter and ultra-cold atom systems.

Contents

1. Introduction

Recently, Majorana fermions in unconventional superconductors and pairing superfluids have become a research focus in condensed matter physics [1–20]. They appear at boundaries and in vortex cores exhibiting non-Abelian statistics which can potentially be used for topological quantum computation [4, 5, 21–25]. Various theoretical schemes have been proposed for the realization and detection of Majorana fermions [9, 14, 15, 26–29], such as the interface between three-dimensional (3D) topological insulators and conventional superconductors [9], the proximity effect of superconductivity in spin–orbit coupled quantum wires [14, 15], Cooper pairing with ultra-cold fermions with synthetic spin–orbit coupling [29] and p-wave Feshbach resonances of single-component ultra-cold fermions [28]. Majorana fermions are also proposed in fractional quantum Hall states at the filling $\nu = \frac{5}{2}$ [30–32]. The signature of the zero energy Majorana boundary mode in the transport spectra has been observed in the spin–orbit coupled quantum wires [16–20].

The boundary Majorana zero modes also appear in unconventional superconductors in two-dimensional (2D) and 3D on edges or surfaces with suitable orientations determined by Cooper pairing symmetries. This is because along the directions of incident and reflected wavevectors of the Bogoliubov quasi-particles, the pairing gap functions have opposite signs [33–35]. These unconventional superconductors can be viewed as weak topological states. They are topologically non-trivial (or trivial) along the directions perpendicular to boundaries with (or without) zero energy modes, respectively.

Interactions can significantly change topological properties of edge and surface in topological insulators and superconductors. For non-chiral systems, these boundary modes are low energy midgap states, thus they are more susceptible to interactions than the gapped bulk states. In the helical edge Luttinger liquids of 2D topological insulators, the edge magnetic fluctuations are much stronger than those in the bulk, which can lead to spontaneous time-reversal symmetry breaking and destroy edge modes [36–38]. For the zero energy boundary Majorana modes along the coupled chains of the p_x-topological superconductors, it has been found that interactions can even generate gaps without breaking time-reversal symmetry in the orbital channel [39]. Similar effects are also found for the helical edge Majorana modes of time-reversal invariant topological pairing states [40, 41]. In both cases, the new topological class under interactions is classified by a Z_8 periodicity.

In this paper, we consider the most natural interaction effects in the boundary states in the p-wave weak topological superconductors or paired superfluids: the coupling between Cooper pairing phases and the zero energy Majorana modes. The degeneracy of these boundary modes is protected by time-reversal symmetry, but is vulnerable under spontaneous time-reversal symmetry breaking in the orbital channel. Spatial variations of phases of Cooper pairing order parameters induce bonding among these boundary modes, and thus lower the energy. Staggered current loops are generated near the boundary, which split the zero energy Majorana peaks. Due to the divergence of the surface density of states, this time-reversal symmetry breaking mechanism is robust.

The rest of this paper is organized as follows. In section 2, we explain the mechanism of spontaneous time-reversal symmetry breaking in the orbital channel with coupled superconducting quantum wires through weak links. In section 3, a 2D p-wave weak topological superconductor is studied with the open boundary condition. The spontaneous staggered orbital current loops appear on the topological non-trivial boundaries, and the consequential splitting of the Majorana zero bias peaks are calculated self-consistently. Experimental realizations of the above effects are discussed in section 4. The summary is presented in section 5.

2. Bonding between boundary Majorana modes

We begin with a heuristic example of two parallel quantum wires along the x-direction. Each of them is a one-dimensional (1D) topological superconductor of single component fermion with p_x-pairing symmetry. As explained in [5], zero energy Majorana modes exist near the two ends of each wire. For example, for the end at $x = L$ of the ith wire ($i = 1, 2$), the operator for the Majorana mode can be expressed as

$$\gamma_i = \int \mathrm{d}x \{u_0(x)\mathrm{e}^{-\mathrm{i}\frac{\theta_i}{2}-\mathrm{i}\frac{\pi}{4}}\psi_i(x) + v_0(x)\mathrm{e}^{\mathrm{i}\frac{\theta_i}{2}+\mathrm{i}\frac{\pi}{4}}\psi_i^\dagger(x)\}, \tag{1}$$

where θ_i is the Cooper pairing phase in the ith chain. We denote Δ the magnitude of the bulk gap, E_f and k_f are the Fermi energy and Fermi momentum, respectively. In the case of $\Delta \ll E_\mathrm{f}$, the zero mode wavefunction is approximated as

$$u_0(x) = v_0(x) \approx \mathrm{e}^{-\frac{L-x}{\xi_x}} \sin k_\mathrm{f} x, \tag{2}$$

where $\xi_x = \frac{2}{k_\mathrm{f}}\frac{E_\mathrm{f}}{\Delta}$ is the coherence length along the x-direction. Now let us connect two right ends with a weak link

$$H_\mathrm{J} = -t_\perp \int_{L-w}^{L} \mathrm{d}x\ [\psi_1^\dagger(x)\psi_2(x) + \mathrm{h.c.}], \tag{3}$$

where w is the width of the link. We assume $w \ll \xi_x$ such that the uniform distribution of the pairing phase within each wire is not affected by the link. By expressing $\psi_i(x) = u_0(x)\mathrm{e}^{\mathrm{i}\frac{\theta_i}{2}+\mathrm{i}\frac{\pi}{4}}\gamma_i + \cdots$ where '$\ldots$' represents for Bogoliubov eigenstates outside the gap Δ, we arrive at two different contributions for the Josephson couplings: the usual one through second-order perturbation process, and the fractionalized one through the zero Majorana mode as

$$E_\mathrm{J} = -J_0 \cos\Delta\theta - \mathrm{i}J_1\gamma_1\gamma_2 \sin\frac{\Delta\theta}{2}, \tag{4}$$

where $\Delta\theta = \theta_1 - \theta_2$, $J \propto t_\perp^2/\Delta$ and $J_1 = t_\perp \int_{L_x-\Delta L}^{L_x} \mathrm{d}x u_0(x)u_0(x+\Delta y)$.

The fractionalized Josephson coupling of the weak link between two wires with the 'head-to-tail' configuration [7, 42] gives rise to $\mathrm{i}\gamma_1\gamma_2\cos\frac{\Delta\theta}{2}$, where $\gamma_{1,2}$ are Majorana modes at two sides of the link. In contrast, for two parallel wires, the corresponding J_1 term in equation (4) is proportional to $\sin\frac{\Delta\theta}{2}$. This difference can be intuitively understood as illustrated in figure 1. We rotate the second wire by 180°, which corresponds to a phase shift of the second wire by π due to the p_x symmetry, and thus $\Delta\theta$ is shifted to $\Delta\theta + \pi$. This changes the dependence of fractionalized Josephson coupling from cosine to sine in equation (4). As a result, the Majorana fermion bonding strength vanishes at $\Delta\theta = 0$ which reflects the fact that these Majorana zero modes are protected by the time-reversal (TR) symmetry in the orbital channel. The bonding strength varies linearly with the phase difference as $\Delta\theta \to 0$, thus equation (4) is minimized at non-zero values of $\Delta\theta_0$ satisfying $\sin\frac{\Delta\theta_0}{2} = \pm\min(\frac{J_1}{4J_0}, 1)$. The energy is gained from the bonding of Majorana fermions. For the general case that $\Delta\theta_0 \neq \pm\pi$, the orbital channel time-reversal symmetry is spontaneously broken. However, in the case of $\frac{J_1}{4J_0} \geqslant 1$, $\Delta\theta_0 = \pm\pi$, the Majorana fermion bonding strength is maximal. Because of the 2π periodicity of phase angles, this case is also TR invariant.

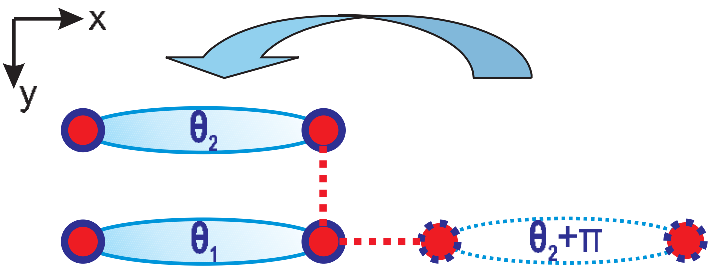

Figure 1. The fractionalized Josephson coupling between two parallel wires through the Majorana zero modes depends on $\sin\frac{\Delta\theta}{2}$ instead of $\cos\frac{\Delta\theta}{2}$. Please note the different orientations of the x and y-directions between figure 2 and this figure.

We can further extend equation (4) to a group of parallel wires whose ends at $x = L$ are weakly connected, which forms 1D or 2D lattices of Majorana modes coupled to the superfluid phases. The effective Hamiltonian is

$$H_{mj} = -J_0 \sum_{\langle ii'\rangle} \cos(\theta_i - \theta_{i'}) - \mathrm{i} J_1 \sum_{\langle ii'\rangle} \sin\frac{\theta_i - \theta_{i'}}{2} \gamma_i \gamma_{i'}, \tag{5}$$

where $\langle ii'\rangle$ refers to the nearest neighbor bonds. The J_0 term favors a global phase coherence with a constant phase value in each wire. However, this results in a flat band of zero energy Majorana fermions which is highly unstable.

In bipartite lattices, a staggered phase configuration $\theta_i = (-)^i \theta'_0$ can minimize the ground state energy by generating a uniform bonding strength, where the value of θ'_0 can be obtained self-consistently. For a 2D lattice of surface Majorana fermions, if the superfluid phase distribution of θ_i forms a vortex, the plaquette in which the vortex core is located exhibit a Z_2 vortex for the Majorana fermion. The motion of the superfluid vortex introduces the dynamic Z_2 flux for the Majorana fermions.

3. Spontaneous staggered orbital currents near the boundary

Having presented the spontaneous orbital channel time-reversal symmetry breaking of Majorana fermions with weak links, now let us consider a 2D superconductor of a single component fermion with the p_x pairing. The bulk of the system with p_x-pairing maintains time-reversal symmetry in the orbital channel unlike the $\mathrm{p}_x + \mathrm{i}p_y$ one in which time-reversal symmetry is broken. We use the tight-binding model of the following mean-field Bogoliubov–de Gennes (B–de G) Hamiltonian with the open boundary condition

$$H_{\mathrm{mf}} = -\sum_i \left\{ (t_x c_i^\dagger c_{i+\hat{e}_x} + t_y c_i^\dagger c_{i+\hat{e}_y} + \mathrm{h.c.}) - \mu c_i^\dagger c_i \right\} - V \sum_i \left\{ \Delta^*_{i,i+\hat{e}_x} c_{i+\hat{e}_x} c_i + \mathrm{h.c.} \right\}$$
$$+ V \sum_i \Delta^*_{i,i+\hat{e}_x} \Delta_{i,i+\hat{e}_x}, \tag{6}$$

where $\Delta_{i,i+\hat{e}_x} = \langle c_{i+\hat{e}_x} c_i \rangle$. In conventional superconductors, the open boundary only affects the magnitude of the pairing order parameter not on the phase distribution. The p_x-type superconductors are weakly topological in 2D, and as is well known, if the phase distribution of $\Delta_{i,i+\hat{e}_x}$ is uniform such that time-reversal symmetry is maintained in the orbital channel, a flat band of Majorana surface modes appear on the boundary along the y-direction.

However, this Majorana band flatness is unstable when the spatial variations of pairing phases are considered. It spontaneously breaks time-reversal symmetry and generates finite bonding strengths among the Majorana modes. Consequently, the macroscopic degeneracy of the surface zero modes is removed and the total energy is lowered. To confirm this intuitive picture, we perform the self-consistent solutions to the B–de G equation (6) at zero temperature. The mean-field Hamiltonian is diagonalized to obtain the Bogoliubov eigenstates whose eigen-operators are defined through $c_i = \sum_n u_n(i)\gamma_n + v_n^*(i)\gamma_n^\dagger$, where $(u_n, v_n)^{\mathrm{T}}$ are the eigenvectors with positive energy eigenvalues $E_n > 0$. The gap equations for $\Delta_{i,i+\hat{e}_x}$ read

$$\Delta_{i,i+\hat{e}_x} = \frac{1}{2}\sum_n \tanh\frac{\beta E_n}{2}\left[u_n(i+\hat{x})v_n^*(i) - v_n^*(i+\hat{x})u_n(i)\right]. \tag{7}$$

The current along the bond between i and $i+\hat{e}_a$ $(a = x, y)$ is

$$j_{i,\hat{e}_a} = -\frac{t_a}{\hbar}\sum_n \mathrm{Im}\,\{v_n(i+\hat{e}_a)v_n^*(i)f(E_n) + u_n(i+\hat{e}_a)u_n^*(i)[1-f(E_n)]\}, \tag{8}$$

where $f(E)$ is the Fermi distribution function.

The spontaneous time-reversal symmetry breaking effect in the orbital channel appears near the boundary normal to the x-direction: circulation current loops as depicted in figure 2(a). As presented in figure 2(b), this edge induces non-uniform phase distribution of the pairing order parameter $\Delta_{i,i+\hat{e}_x}$. However, it is non-singular which does not exhibit the vortex configuration and thus cannot give rise to the current loops by itself. Loosely speaking there are two different contributions to the current expression of equation (8): the Bogoliubov modes whose energies outside the bulk gap, and the in-gap states of Majorana modes. The former contribution can be captured by the Ginzburg–Landau formalism as spatial phase variations of $\Delta_{i,i+\hat{e}_x}$, while the latter arises from Majorana modes cannot. The circulation pattern of these induced edge currents are staggered, which is natural, since in the background of superfluidity the overall vorticity should be neutral in the absence of external magnetic fields. The size of current loops should be at the order of coherence lengths which can be estimated as $\xi_a/a_0 \approx 2t_a/\Delta$ with $a = x, y$ where a_0 is the lattice constant. Currents decay exponentially along the x-direction at the scale of ξ_x, and change directions along the y-direction at the scale of $2\xi_y$.

Next we calculate the local density of states (LDOS) near the boundary as depicted in figure 3. The expression for LDOS reads

$$L(i,\omega) = \sum_n |u_n(i)|^2\delta(\omega - E_n) + |v_n(i)|^2\delta(\omega + E_n). \tag{9}$$

For comparison, we first present the result without self-consistency in figure 3(a) by fixing order parameters $\Delta_{i,i+\hat{e}_x}$ uniform with the bulk value. The central peak at zero energy represents the edge Majorana states. However, with self-consistency, spatial variations of $\Delta_{i,i+\hat{e}_x}$ couple to the edge Majorana modes. The zero energy peaks are split as depicted in figures 3(b)–(d). Sites 2 and 3 (figures 3(b) and (c), respectively) are right on the boundary normal to x-direction, and thus their coherence peaks are strongly suppressed. Site 4 (figure 3(d) is relatively inside, and thus the midgap peaks are suppressed. Site 2 locates in the middle of current loops, and thus the splitting of the zero bias peak is the largest.

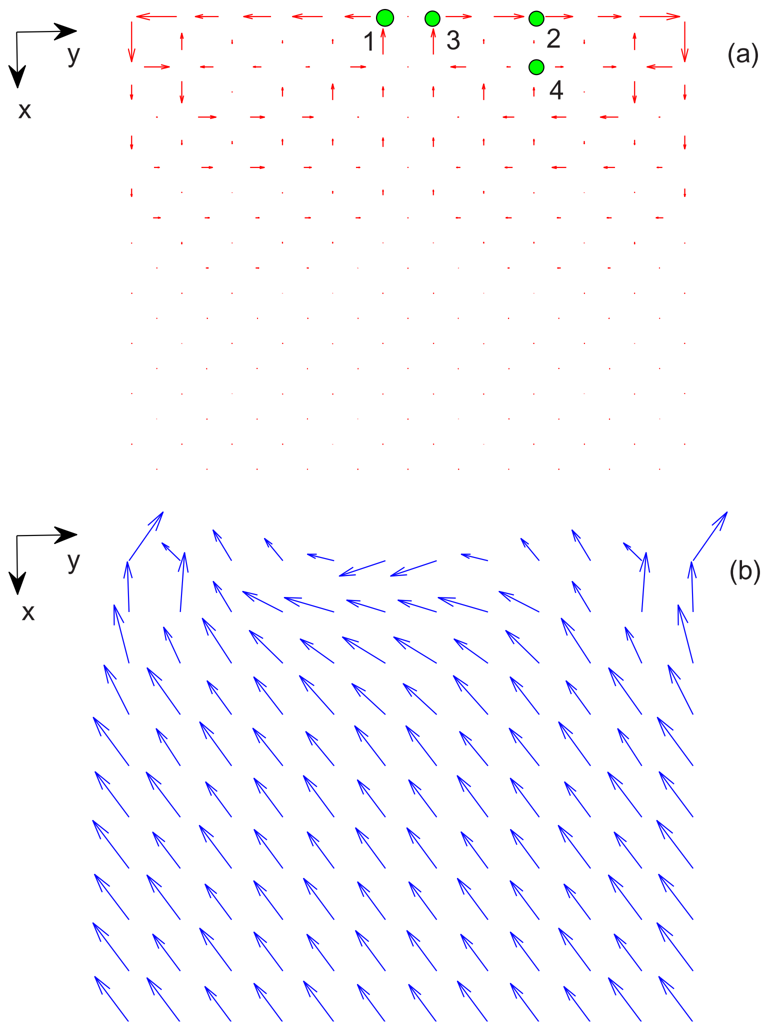

Figure 2. The current and phase distributions from the self-consistent solutions to equation (6) with the open boundary condition. The system size is $L_x \times L_y$ with $L_x = 20$ and $L_y = 12$, and parameter values $t_x = 1$, $t_y = 1.2$, $V = 3$ and $\mu = 0$. Only half of the system along the x-direction is depicted, and the distributions in the rest half can be obtained by performing the reflection operation. (a) The spontaneously generated edge current distributions; (b) the lengths and directions of arrows represent magnitudes and phase angles $\theta_{i,i+\hat{e}_x}$ for the pairing operators $\Delta_{i,i+\hat{e}_x}$, respectively.

Due to the divergence of density of states at zero energy, the above time-reversal symmetry breaking mechanism in the orbital channel is general. It also applies to the 3D case with the p_z-pairing. Then the xy-surface is non-trivial along which Majorana zero energy flat bands appear with the assumption of time-reversal symmetry. Again due to the same reasoning, this degeneracy will be lifted by spontaneous TR symmetry breaking. In this case, we expect that the 2D vortex–anti-vortex pattern in figure 2 will change to that of 3D closed vortex rings, which may further form a lattice structure parallel to the xy-surface. Further study of this lattice structure will be deferred to a later publication. Moreover, the above physics also applies in the continuum not just in the tight-binding model. Staggered vortices or closed vortex rings will

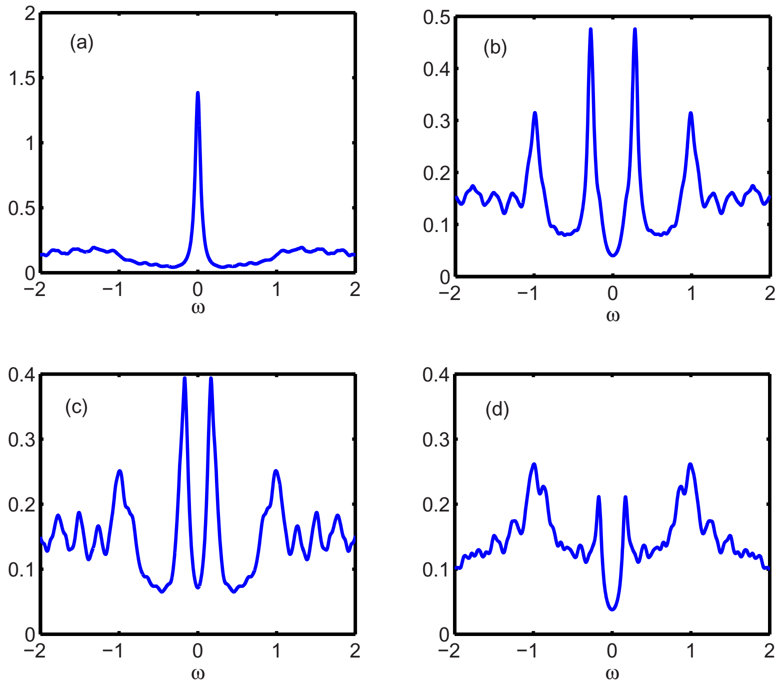

Figure 3. The edge LDOS spectra for the system in figure 2 $\delta(\omega \pm E_n)$ in equation (9) are approximated by $\frac{1}{\pi}\eta/[(\omega \pm E_n)^2 + \eta^2]$ with the broadening parameter $\eta = 0.04$. Panels (a)–(d) are the LDOS spectra at points 1–4 marked in figure 2(a), respectively. (a) LDOS without self-consistency by fixing $\Delta_{i,i+\hat{e}_x}$ at a uniform bulk value. Panels (b)–(d) are self-consistent results. The corresponding parameter values are presented in the caption of figure 2.

appear near the edge or surfaces within the size of coherence lengths, which will also split the zero energy peaks of Majorana fermions.

Next we briefly discuss the boundary Majorana flat bands for the TR invariant spinful p_x-wave Cooper pairing. For example, let us consider the pairing order parameter in the bulk as $\Delta_{i,i+e_x} = \mathrm{i}|\Delta|\sigma_2\vec{\sigma}\cdot\vec{d}$. Without loss of generality, we can assume that the d-vector lies in the xy-plane with the azimuthal angle ϕ, i.e. $d_x + \mathrm{i}d_y = |d|\mathrm{e}^{\mathrm{i}\phi}$. This corresponds to that spin-up fermions are paired with spin-up, and spin-down ones are paired with spin-down, with the relation $\Delta_{\uparrow\uparrow} = |\Delta|\mathrm{e}^{\mathrm{i}\phi}$ and $\Delta_{\downarrow\downarrow} = |\Delta|\mathrm{e}^{-\mathrm{i}\phi}$. Then the boundary Majorana modes consist of two branches $\gamma_\uparrow$ and $\gamma_\downarrow$ forming Kramer pairs. The bonding among Majorana modes can occur within each branch of Kramer pair by developing currents as explained above. If a residue magnetic interaction exists, another way to remove the degeneracy is to develop magnetism with the order parameter $\mathrm{i}\gamma_\uparrow\gamma_\downarrow$. The spin polarization for such an order is in the xy-plane. In general, these two different bonding mechanisms can coexist.

4. Discussions

The above real p-wave Cooper pairing of single component fermion can be realized in ultra-cold dipolar fermionic molecular systems. For example, the ^{40}K–^{87}Rb systems have been cooled down below quantum degeneracy [43, 44]. Moreover, the chemically stable dipolar fermion molecules of ^{23}Na–^{40}K have also been laser-cooled [45]. If the dipole moments are aligned along the z-axis by external electric fields, the interaction between two dipole moments exhibits the $d_{r^2-3z^2}$-type anisotropy. It means that the interaction is attractive if the displacement vector between two dipoles is along the z-axis, and repulsive if it lies in the xy-plane. Naturally, this leads to the p_z-type Cooper pairing in the strong coupling limit. Even in the weak coupling limit, partial wave analysis also shows that the dominant pairing symmetry is the p_z-type. Due to the anisotropy of the interaction, it slightly hybridizes with other odd partial wave channels as predicted in previous works [46–48]. For the two-component dipolar fermions, the triplet p_z Cooper pairing has also been theoretically predicted [49, 50]. The above predicted spontaneous time-reversal symmetry breaking effects in the orbital channel will appear on the surfaces perpendicular to the z-axis.

In the condensed matter systems, the boundary Majorana fermion has been detected in the 1D quantum wire with spin–orbit coupling [16–20]. A magnetic field is also applied in parallel to the wire to lift the degeneracy at zero momentum such that the system is effectively one component if the Fermi energy lies inside the gap. In this case, the major effect of the magnetic field is the Zeeman effect, and the time-reversal symmetry is not explicitly broken in the orbital channel. The proximity effect from the superconducting electrodes induces superconductivity in the 1D wire, which leads to the zero energy Majorana ending states. If we put an array of these 1D wires together and their ends are weakly connected, these Majorana modes will also spontaneously build up bonding strength by developing staggered orbital currents patterns, the consequential splitting of the zero bias peaks will be exhibited in the tunneling spectroscopy.

5. Conclusion

In summary, we have found that the zero energy boundary Majorana flat bands of the p-wave superconductors are unstable toward spontaneous time-reversal symmetry breaking in the orbital channel, which results from the coupling between Majorana modes and the Cooper pairing phases. The divergence of density of states at zero energy leads to spontaneous formation of staggered current loops, which generates bondings among the Majorana modes and lifts the degeneracy. This is a robust mechanism which appears even without introducing new instabilities.

Acknowledgments

We thank Z Cai for early collaboration on this work, and J Alicea, L Fu, B Halperin, and P A Lee for helpful discussions. YL, DW and CW are supported by the NSF DMR-1105945 and AFOSR FA9550-11-1- 0067(YIP); YL is also supported by the Inamori Fellowship.

Note added. Part of this work was presented in the 2011 APS March meeting [51]. Near the completion of this paper, we learned of the nice work [52], which studies the magnetic instabilities in Majorana flat bands.

References

[1] Kopnin N B and Salomaa M M 1991 Mutual friction in superfluid ^{3}He: effects of bound states in the vortex core *Phys. Rev.* B **44** 9667–77

[2] Volovik G E 1999 Fermion zero modes on vortices in chiral superconductors *J. Exp. Theor. Phys. Lett.* **70** 609–14

[3] Read N and Green D 2000 Paired states of fermions in two dimensions with breaking of parity and time-reversal symmetries and the fractional quantum Hall effect *Phys. Rev.* B **61** 10267–97

[4] Ivanov D A 2001 Non-abelian statistics of half-quantum vortices in p-wave superconductors *Phys. Rev. Lett.* **86** 268–71

[5] Kitaev A Y 2001 Unpaired Majorana fermions in quantum wires *Phys.—Usp.* **44** 131

[6] Sengupta K, Žutić I, Kwon H-J, Yakovenko V M and Das Sarma S 2001 Midgap edge states and pairing symmetry of quasi-one-dimensional organic superconductors *Phys. Rev.* B **63** 144531

[7] Kwon H-J, Sengupta K and Yakovenko V M 2004 Fractional ac Josephson effect in p- and d-wave superconductors *Eur. Phys. J.* B **37** 349–61

[8] Stone M and Chung S-B 2006 Fusion rules and vortices in $p_x + \mathrm{i}p_y$ superconductors *Phys. Rev.* B **73** 014505

[9] Fu L and Kane C L 2008 Superconducting proximity effect and Majorana fermions at the surface of a topological insulator *Phys. Rev. Lett.* **100** 096407

[10] Fu L and Kane C L 2009 Josephson current and noise at a superconductor/quantum-spin-Hall-insulator/superconductor junction *Phys. Rev.* B **79** 161408

[11] Qi X-L, Hughes T L, Raghu S and Zhang S-C 2009 Time-reversal-invariant topological superconductors and superfluids in two and three dimensions *Phys. Rev. Lett.* **102** 187001

[12] Cheng M, Lutchyn R M, Galitski V and Das Sarma S 2009 Splitting of Majorana-fermion modes due to intervortex tunneling in a $p_x + \mathrm{i}p_y$ superconductor *Phys. Rev. Lett.* **103** 107001

[13] Chung S B and Zhang S-C 2009 Detecting the Majorana fermion surface state of $^3\mathrm{He}_b$ through spin relaxation *Phys. Rev. Lett.* **103** 235301

[14] Sau J D, Lutchyn R M, Tewari S and Das Sarma S 2010 Generic new platform for topological quantum computation using semiconductor heterostructures *Phys. Rev. Lett.* **104** 040502

[15] Sau J D, Tewari S, Lutchyn R M, Stanescu T D and Das Sarma S 2010 Non-abelian quantum order in spin–orbit-coupled semiconductors: search for topological Majorana particles in solid-state systems *Phys. Rev.* B **82** 214509

[16] Mourik V, Zuo K, Frolov S M, Plissard S R, Bakkers E P A M and Kouwenhoven L P 2012 Signatures of Majorana fermions in hybrid superconductor–semiconductor nanowire devices *Science* **336** 1003–7

[17] Churchill H O H, Fatemi V, Grove-Rasmussen K, Deng M T, Caroff P, Xu H Q and Marcus C M 2013 Superconductor-nanowire devices from tunneling to the multichannel regime: zero-bias oscillations and magnetoconductance crossover *Phys. Rev.* B **87** 241401(R)

[18] Das A, Ronen Y, Most Y, Oreg Y, Heiblum M and Shtrikman H 2012 Zero-bias peaks and splitting in an Al–InAs nanowire topological superconductor as a signature of Majorana fermions *Nature Phys.* **8** 887–95

[19] Finck A D K, Van Harlingen D J, Mohseni P K, Jung K and Li X 2013 Anomalous modulation of a zero-bias peak in a hybrid nanowire-superconductor device *Phys. Rev. Lett.* **110** 126406

[20] Rokhinson L P, Liu X and Furdyna J K 2012 The fractional ac Josephson effect in a semiconductor–superconductor nanowire as a signature of Majorana particles *Nature Phys.* **8** 795–9

[21] Teo J C Y and Kane C L 2010 Majorana fermions and non-abelian statistics in three dimensions *Phys. Rev. Lett.* **104** 046401

[22] Freedman M, Hastings M B, Nayak C, Qi X-L, Walker K and Wang Z 2011 Projective ribbon permutation statistics: a remnant of non-abelian braiding in higher dimensions *Phys. Rev.* B **83** 115132

[23] Alicea J, Oreg Y, Refael G, von Oppen F and Fisher M P A 2011 Non-abelian statistics and topological quantum information processing in 1D wire networks *Nature Phys.* **7** 412–7

[24] Jiang L, Kane C L and Preskill J 2011 Interface between topological and superconducting qubits *Phys. Rev. Lett.* **106** 130504

[25] Halperin B I, Oreg Y, Stern A, Refael G, Alicea J and von Oppen F 2012 Adiabatic manipulations of Majorana fermions in a three-dimensional network of quantum wires *Phys. Rev.* B **85** 144501

[26] Stanescu T D and Tewari S 2013 Majorana fermions in semiconductor nanowires: fundamentals, modeling and experiment *J. Phys.: Condens. Matter* **25** 233201

[27] Alicea J 2012 New directions in the pursuit of Majorana fermions in solid state systems *Rep. Prog. Phys.* **75** 076501

[28] Gurarie V and Radzihovsky L 2007 Resonantly paired fermionic superfluids *Ann. Phys.* **322** 2–119
[29] Zhang C, Tewari S, Lutchyn R M and Das Sarma S 2008 $p_x + \mathrm{i}p_y$ superfluid from s-wave interactions of fermionic cold atoms *Phys. Rev. Lett.* **101** 160401
[30] Das Sarma S, Freedman M and Nayak C 2005 Topologically protected qubits from a possible non-abelian fractional quantum Hall state *Phys. Rev. Lett.* **94** 166802
[31] Stern A and Halperin B I 2006 Proposed experiments to probe the non-abelian $\nu = 5/2$ quantum Hall state *Phys. Rev. Lett.* **96** 016802
[32] Nayak C, Simon S H, Stern A, Freedman M and Das Sarma S 2008 Non-abelian anyons and topological quantum computation *Rev. Mod. Phys.* **80** 1083–159
[33] Hu C-R 1994 Midgap surface states as a novel signature for d^2_{xa}-x^2_b-wave superconductivity *Phys. Rev. Lett.* **72** 1526–9
[34] Tanaka Y and Kashiwaya S 1995 Theory of tunneling spectroscopy of d-wave superconductors *Phys. Rev. Lett.* **74** 3451–4
[35] Kashiwaya S and Tanaka Y 2000 Tunnelling effects on surface bound states in unconventional superconductors *Rep. Prog. Phys.* **63** 1641
[36] Wu C, Andrei Bernevig B and Zhang S-C 2006 Helical liquid and the edge of quantum spin Hall systems *Phys. Rev. Lett.* **96** 106401
[37] Xu C and Moore J E 2006 Stability of the quantum spin Hall effect: effects of interactions, disorder and $\mathbb{Z}_2$ topology *Phys. Rev.* B **73** 045322
[38] Zheng D, Zhang G-M and Wu C 2011 Particle–hole symmetry and interaction effects in the Kane–Mele–Hubbard model *Phys. Rev.* B **84** 205121
[39] Fidkowski L and Kitaev A 2011 Topological phases of fermions in one dimension *Phys. Rev.* B **83** 075103
[40] Yao H and Ryu S 2012 Interaction effect on topological classification of superconductors in two dimensions arXiv:1202.5805
[41] Qi X-L 2013 A new class of $(2+1)$-d topological superconductor with $\mathbb{Z}_8$ topological classification *New J. Phys.* **15** 065002
[42] Xu C and Fu L 2010 Fractionalization in Josephson junction arrays hinged by quantum spin Hall edges *Phys. Rev.* B **81** 134435
[43] Ni K-K, Ospelkaus S, Wang D, Quéméner G, Neyenhuis B, de Miranda M H G, Bohn J L, Ye J and Jin D S 2010 Dipolar collisions of polar molecules in the quantum regime *Nature* **464** 1324–8
[44] Ospelkaus S, Ni K-K, Wang D, de Miranda M H G, Neyenhuis B, Quéméner G, Julienne P S, Bohn J L, Jin D S and Ye J 2010 Quantum-state controlled chemical reactions of ultracold potassium–rubidium molecules *Science* **327** 853
[45] Wu C-H, Park J W, Ahmadi P, Will S and Zwierlein M W 2012 Ultracold fermionic Feshbach molecules of $Na_{23}K_{40}$ *Phys. Rev. Lett.* **109** 085301
[46] Baranov M A, Mar'enko M S, Rychkov V S and Shlyapnikov G V 2002 Superfluid pairing in a polarized dipolar fermi gas *Phys. Rev.* A **66** 013606
[47] Baranov M A, Dobrek Ł and Lewenstein M 2004 Superfluidity of trapped dipolar fermi gases *Phys. Rev. Lett.* **92** 250403
[48] You L and Marinescu M 1999 Prospects for p-wave paired Bardeen–Cooper–Schrieffer states of fermionic atoms *Phys. Rev.* A **60** 2324
[49] Wu C and Hirsch J E 2010 Mixed triplet and singlet pairing in ultracold multicomponent fermion systems with dipolar interactions *Phys. Rev.* B **81** 020508
[50] Shi T, Zhang J-N, Sun C-P and Yi S 2010 Singlet and triplet Bardeen–Cooper–Schrieffer pairs in a gas of two-species fermionic polar molecules *Phys. Rev.* A **82** 033623
[51] Li Y and Wu C 2011 *Bull. Am. Phys. Soc.* 56 see http://physics.ucsd.edu/~y4li/talks/11APS.ppt
[52] Potter A C and Lee P A 2013 Edge-ferromagnetism from Majorana flat-bands: application to split tunneling-conductance peaks in the high-tc cuprates arXiv:1303.6956